Yttrium Iron Garnet/Barium Titanate Multiferroic Composites

SCHILEO, Giorgio, GONZALEZ, Cristina Pascual, ALGUERO, Miguel, REANEY, Ian M, POSTOLACHE, Petronel, MITOSERIU, Liliana, REICHMANN, Klaus and FETEIRA, Antonio <http://orcid.org/0000-0001-8151-7009>

Published version

SCHILEO, Giorgio, GONZALEZ, Cristina Pascual, ALGUERO, Miguel, REANEY, Ian M, POSTOLACHE, Petronel, MITOSERIU, Liliana, REICHMANN, Klaus and FETEIRA, Antonio (2016). Yttrium Iron Garnet/Barium Titanate Multiferroic Composites. Journal of the American Ceramic Society, 99 (5), 1609-1614.

Yttrium Iron Garnet/Barium Titanate Multiferroic Composites

Giorgio Schileo[1], *Cristina Pascual Gonzalez*[1], *Miguel Alguero*[2], *Ian M. Reaney*[3], *Petronel Postolache*[4], *Liliana Mitoseriu*[4], *Klaus Reichmann*[5] *and Antonio Feteira*[1]

[1]Christian Doppler Laboratory on Advanced Ferroic Oxides, Sheffield Hallam University, Howard Street, Sheffield, S1 1WB, UK

[2]Instituto de Ciência de Materiales de Madrid, CSIC, Cantoblanco 28049, Madrid, Spain

[3]University of Sheffield, Department of Materials Science and Engineering, Sir Robert Hadfield Building, Mappin Street, Sheffield, S1 3JD, UK

[4]A.I. Cuza University, Faculty of Physics, Blvd. Carol I 11, 700506, Iasi, Romania

[5]Christian Doppler Laboratory on Advanced Ferroic Oxides, , Institute for Chemistry and Technology of Materials, Graz University of Technology, Stremayrgasse 9, 8010, Graz, Austria

Abstract

Dense multiferroic 0-3 type composites encompassing $BaTiO_3$ and $Y_3Fe_5O_{12}$ were fabricated by the solid state reaction method. X-ray diffraction data combined with Scanning Electron Microscopy imaging show virtual immiscibility between the two phases, with the $Y_3Fe_5O_{12}$ ferrimagnetic phase well dispersed in the tetragonal $BaTiO_3$ ferroelectric matrix. Raman spectroscopy analyses corroborate the polar nature of the $BaTiO_3$ matrix in composites with a $Y_3Fe_5O_{12}$ content as great as 40 wt%. Ferrimagnetism is detected in all composites and no additional magnetic phases are distinguished. Although these dense ceramics can be electrically poled, they exhibit a very weak magnetoelectric response, which slightly increases with $Y_3Fe_5O_{12}$ content.

Introduction

Magnetoelectric Multiferroics (MFs) are multifunctional materials which display simultaneously ferroelectric and magnetic order, and coupling between these two order parameters, i.e. the polarisation can be manipulated by a magnetic field, and likewise the magnetisation by an electric field. This phenomenon is referred to as the magnetoelectric (ME) effect, and its potential development may have a huge impact on the electronic industry, since they would enable us to develop 4-state logic memories, electrically written magnetic data, new tuneable sensors and transducers, to name but a few.[1, 2] The search for single-phase materials dates back to the 1960s, when doping ferroelectric crystals with magnetic ions was intensively investigated and often showed that ferroelectricity would vanish even without the establishment of magnetic ordering. Nowadays there are more than 20 single-phase MFs, however the coexistence of both ferroic properties is only observed at cryogenic temperatures. Two of the main reasons why a feasible single-phase MF has not been discovered yet are a) the fact that ferroelectricity, in most ferroelectrics such as $BaTiO_3$, depends on the hybridisation of empty d orbitals of Ti with p orbitals of oxygen atoms, whereas magnetism arises from unpaired electrons in the same shells; b) magnetic cations, because of their unpaired electrons, are also relatively good conductors compared to ferroelectrics, therefore because of the increased conductivity it is then it is then impossible to apply large electric fields and ferroelectric properties are lost.[3] The theoretical understanding of these and other reasons moved the attention to composite materials.

In composites, each ferroic property is carried by a separate phase, chosen in order to be ferroelectric and ferromagnetic, respectively. The ferroelectric phase, which it is also piezoelectric can generate a strain that is passed onto a magnetostrictive phase, which in turn develops magnetisation, and vice versa. Basically, the ME effect is a result of the product of the magnetostrictive effect (i.e. a magnetic/mechanical effect) from magnetic phase and the piezoelectric effect (i.e. a mechanical/electrical effect) from the piezoelectric phase, given either as[4]:

$$ME_H effect = \frac{magnetic}{mechanical} \times \frac{mechanical}{electric}$$

or

$$ME_H effect = \frac{electric}{mechanical} \times \frac{mechanical}{magnetic}$$

The two phases can be arranged according to various geometries. Newnham et al[5] introduced a phase connectivity concept to describe the structure of two-phase composites using the following notations: 0-3 for one-phase particles (denoted as 0) embedded in a matrix (denoted as 3), 2-2 for multilayer materials or 1-3 for tubes, pillars and other elongated structures embedded into a matrix. In any case, the ME coupling is achieved via mechanical strain. A good contact between the surfaces of the two phases is therefore essential to transfer the strain and achieve a useful ME effect (> 20 mV cm^{-1} Oe^{-1}).[4]

In our previous work, we compared two sol-gel methods and a coprecipitation method to prepare 0-3 composite ceramics of $BaTiO_3$ (BT) and $Y_3Fe_5O_{12}$ (YIG)[6]. YIG was chosen in place of $CoFe_2O_4$ due to its much higher electrical resistance and the possibility of its use at high frequencies. The results showed that the coprecipitation method was the most suitable to retain ferroelectricity in the sintered composite. However, issues such as low density and aggregation of YIG persisted: low density is detrimental to ferroelectric properties, and aggregation reduces the interface area between the magnetic and the ferroelectric phase. Therefore, in this study we prepared particulate composites in 0-3 geometry of BT and YIG by solid state reaction method, with the aim of improving density and reducing YIG aggregation, as previously observed by Schileo et al[6]. Moreover, the concentration of YIG is varied to identify the percolation threshold for DC current under an electric field.

Experimental

BT was prepared by solid state reaction method. Starting reagents $BaCO_3$ and TiO_2 (Sigma Aldrich, UK, ACS reagent, >99%) were mixed in polypropylene (PP) bottles with yttria-stabilised zirconia milling media and propan-2-ol as solvent and milled overnight. The obtained slurries were dried, sieved through a 250 mesh stainless steel sieve and calcined at 800, 900, 1000 and 1100 ºC for 8 hours. YIG was also prepared by the same method from Fe_2O_3 and Y_2O_3 (Sigma Aldrich, UK, ACS

reagent, >99%), and the mixed powders were reacted at 900 and 1200 ºC. The powders were then mixed and ball milled together with 2 wt% polyethylene glycol (PEG) as binder to produce four compositions: 10, 20, 30 and 40 wt% of YIG in BT. As a reference, pellets of BT and YIG were also prepared. Green bodies were pressed isostatically at 200 MPa, heated at 1 ºC/min to 500 ºC for 5 hours to remove the binder and finally sintered at 1300 ºC for 2 hours. To fabricate electrodes, Pt paste was applied to the faces of the pellets and fired at 700 ºC for 30 min.

Purity and phase contents were studied using an X-ray diffractometer in reflection geometry (model: Empyrean, Panalytical™, Almelo, The Netherlands, $K_{\alpha 1}$-Cu line at λ = 1.54060 Å and step size 0.0130º [2θ]). The composites microstructures were investigated using a Scanning electron Microscope (SEM) (model: Nova Nano 200 with Field Emission Gun, FEI, Brno, Czech Republic). Lattice parameters were calculated using the X'Pert High Score software suite. The sintered composites were ground using SiC paper, polished using 6 and 1 µm-diamond suspension, and then coated with carbon. Raman spectra were obtained in back-scattering geometry using a Raman microscope (model: In Via, Renishaw, Glouchestershire, UK) using an Ar laser at 514.5 nm and 10 mW. Magnetic hysteresis loops were measured using a SVM (Sample vibrating Magnetometer, Princeton Measurements Corporation, Princeton, NJ, USA) coupled with a Micromag^{TM} furnace vacuum monitor and gas flow controller (Princeton Measurements Corporation, Princeton, NJ, USA). The instrument is calibrated daily using an Yttrium Iron Garnet sphere ($7.825 \cdot 10^{-2}$ emu, NIST standard reference material no. 2853). Dielectric properties were measured with an Impedance/Gain Phase Analyser (model: 1260, Solartron instruments, Farnborough, UK) connected to a Carbolite™ (Hope Valley, UK) tube furnace. Capacitance was measured versus temperature (from room temperature to 250 °C, 1 °C/min) at five different frequencies (1, 10, 100, 250 and 1000 kHz). The ferroelectric hysteresis loops were taken using a ferroelectric tester (model: RT60, Radiant Technologies, Albuquerque, New Mexico, USA).

Composites were heated up to 100 °C in silicone oil for 1 h under 20 kV/cm, and subsequently cooled naturally to room temperature maintaining the same electric field, before magnetoelectric characterization. This was carried out with a system consisting of two Helmholtz coils (Serviciencia

S.L., Spain): a high power and a high frequency coil, designed to independently provide a static magnetic field up to 1 kOe (to magnetize the material), and an alternate magnetic field up to 10 Oe at 10 kHz (the stimulus). Magnetoelectric out-put voltages were monitored with a lock-in amplifier (model 7265 Signal Recovery, TN, USA).

Results

Fig. 1 shows the room temperature X-ray diffraction data of BT, BT-YIG composites ceramics (YIG = 10-40 wt%) and YIG, sintered at 1300 ºC for 2 h. BT ceramics are single phase and as expected their crystal symmetry is well described by the tetragonal space group $P4mm$, as evidenced by the 002/200 doublet. A small amount of $YFeO_3$ (yttrium orthoferrite, PDF no. 00-039-1489) is observable in YIG, due to the equilibrium:

$$Y_3Fe_5O_{12} \leftrightarrow 3YFeO_3 + Fe_2O_3 \qquad \text{(eq. 1)}$$

Small amounts of the parasitic phases $Y_2Ti_2O_7$ (PDF no. 00-042-0413) and possibly $BaFe_{12}O_{19}$ (PDF no. 00-039-1433) are also present in the composites, as indicated by the reflections at 30.3 º2θ (for $BaFe_{12}O_{19}$) and 30.7 º2θ (for $Y_2Ti_2O_7$ and $BaFe_{12}O_{19}$), due to reaction at the interfaces between BT and YIG. The degree of tetragonality decreases in the composites as compared to pure BT (1.0106), ranging from 1.004 to 1.006 (Table 1). An exception to this trend it is observed for the 20 wt% composites, which exhibits the lowest c/a ratio. Also the XRD data for the 30 wt% composites shows asymmetric peaks for both phases. At this stage we can only speculate that this asymmetry can either be an artefact from the measurement or residual strain on the composite.

Fig. 2 shows the back-scattered electron images of the polished surface for all ceramic composites. All composites exhibit high relative density, between 96% and 98%, as corroborated by the almost complete absence of porosity, especially for low YIG concentrations. YIG grains range in size from 1 to 2 μm and are also well dispersed within the BT matrix; the formation of significantly large aggregates does not occur until YIG = 40 wt%, where the level of porosity is also slightly larger.

The Raman spectra for YIG and for each composite are shown in Fig. 3 (polished sintered pellets). All modes can be assigned to either the YIG or BT phase. YIG presents the same general features as spectra reported in the literature[7]; polycrystalline BT presents three broad modes at ~260, ~510 and ~720 cm^{-1}, and a sharp mode at ~307 cm^{-1}. YIG instead presents several sharp modes at 129, 170, 192, 235, 270 (the most intense), 340, 374, 415, 443, 504, 585, 676, 703 and 733 cm^{-1}, and a broader band at ~890 $cm^{-1,}$ labelled from 0 to 14. The intensity of YIG modes increases with YIG concentration in the composites, and there is no appreciable shift in mode positions in relation to the pure compound. Moreover, no additional modes due to parasitic phases are observed. Nevertheless, the A_1 (TO) (~250 cm^{-1})[8] for BT shifts towards lower frequencies, which may be indicative of residual strain.[9]

Fig. 4 shows the temperature dependence of relative permittivity and dielectric loss for composites sintered at 1300 ºC for 2 h. The room temperature relative permittivity, ε_r, for the composites is ~1400 (10 wt% YIG), ~1250 (20 wt% YIG), ~1000 (30 wt% YIG) and ~300 (40 wt% YIG), respectively, at 1 MHz. All composites show a dielectric anomaly around 120-130 ºC, which is associated with the paraelectric-to-ferroelectric transition of BT. The maximum associated to the phase transition becomes broader and less intense with increasing YIG. Above this temperature, ε_r decays continuously, however, for YIG = 30 and 40 wt% we can observe a strong frequency dispersion and increased loss at room temperature (20 - 30%), whereas for YIG = 10 and 20 wt% dielectric loss is very low for this type of particulate composite, being as low as 3-5% up to 150 ºC. On heating, the permittivity continues to increase due to the enhanced conductivity, but this occurs above ~250 ºC for 10 and 20 wt% YIG and already above ~150 ºC for 30 and 40 wt% YIG. The dielectric losses increase with increasing temperature as a result of increased electrical conductivity.

The PE loops (Fig. 5) reveal a good insulating behaviour of composites with a YIG content up to 30 wt%. Indeed, those composites are resistive enough to withstand a 40 kV cm^{-1} electric field. However, even under such high fields, the recorded PE loops are unsaturated and strongly affected by resistive losses, in particular for composites with 40 wt% YIG, as shown in Fig. 5. Hence, for YIG concentrations of 10 and 20 wt%, the PE loops indicate a sub-switching regime (Rayleigh), which makes impossible to describe by quantitative characteristics (remanent polarisation, coercive field) the

switching character of these composites. Nevertheless, these PE loops clearly show the composites with a YIG content up to 30 wt% to sustain electric fields as high as 40 kV cm^{-1}. The room temperature polarisation (non-saturated) for these composites reaches 5 to 6 μC cm^{-2} under an applied field of 40 kV.cm^{-1}.

Fig. 6 shows the magnetic hysteresis loops for the ceramic composites from -10 kOe to +10 kOe. The saturation magnetisation (M_S) of YIG ceramics is 24.7 emu/g, whereas for composites M_S varies as follows: 1.48 emu/g (YIG = 10 wt%), 4.14 emu/g (YIG = 20 wt%), 6.87 emu/g (YIG = 30 wt%), and 10.51 emu/g (YIG = 40 wt%); at 10 wt%, YIG also shows higher coercivity (80 Oe) than for higher concentrations (10-15 Oe), the latter being closer to the value for isolated YIG (~16 Oe).

Linear longitudinal magnetoelectric coefficients α_{33} are given in Fig. 7. Note the characteristic dependence with the static magnetic field, typical of magnetoelectric composites. Maximum values of ≈ 24, 40 and 60 μV cm^{-1} Oe^{-1} are achieved for composites with 10, 20 and 30 wt% YIG content, at an increasing static magnetic field of ≈ 330, 370 and 520 Oe, respectively.

Discussion

First, XRD from these composites shows evidence of smaller amounts of parasitic phases in relation to those prepared by sol-gel methods[6] and the crystal structure of BT is clearly tetragonal. The *c/a* ratio for BT in the composites is approximately 1.005, which is smaller than the value of 1.0106 measured for BT ceramics. In principle, significant chemical doping associated with a potential diffusion of either Y or Fe into the BT lattice can be ruled out, because the Curie temperature does not show any shift. YIG lattice parameters also show good agreement with the literature values.

Second, SEM images show very dense ceramics, a fundamental prerequisite for an effective ME coupling via strain in multiferroic composites. Back-scattered electron images of the sintered composites failed to reveal evidence of parasitic phases in the observed areas, despite their detection in the XRD experiments.

Third, it is important to note the presence of a peak at 307 cm^{-1} in the Raman spectra of all composites, which is ascribed to the E(TO+LO) mode (Fig. 3): this mode is generally regarded as a "signature" for the presence of ferroelectricity in BT. The Raman spectra of the composites show no evidence of parasitic phases or doping, such as extra modes, for BT. Nevertheless, Nevertheless, the A_1 (TO) (~250 cm^{-1}) for BT shifts towards lower frequencies, which may be indicative of residual strain. This is due to the local scale of the Raman probe, compared to the average picture given by XRD.[9, 10, 11] Nevertheless, it is worth to mention that the XRD reflections for 30 wt% composite are asymmetric, which is also consistent with residual strain. The assignment of Raman mode 0 at 129 cm^{-1} to the YIG phase (uncertain in our previous work[6]) is confirmed by comparing the Raman spectra of isolated YIG and that of composite with x = 0.30 and 0.40. The mode appears only at higher concentration and its intensity relative to modes 1 and 2 in the composites matches the relative intensity in the isolated YIG. Finally, the dielectric anomaly related to the ferroelectric-to-paraelectric transition in BT is present in all composites, with relatively low loss up to 20 wt% YIG, together with high permittivity, due to the high resistivity of YIG; as a comparison, particulate composites of BT and $CoFe_2O_4$ show dielectric loss as high as 15-20% for 20 wt% $CoFe_2O_4$ in BT[12]. Furthermore, at least 40 kV/cm can be applied to our composites (up to 30 wt% YIG) without dielectric breakdown due to DC conductivity (fig. 5), a better result than that obtained, for example, by combining just 10 wt% $BaFe_{12}O_{19}$ in BT[13], where the maximum applicable voltage was 2.5 kV cm^{-1}, or 35 wt% $CoFe_2O_4$, again with BT[14], where 25 kV cm^{-1} corresponds to a maximum polarisation of ~4 μC cm^{-2}.

In theory, the relative permittivity in composites can be estimated from empirical expressions which combine the permittivity of each component phase and their relative concentrations. Hence, considering the relative permittivity of YIG, measured at room temperature and 1 MHz, to be 14, which is in agreement with the literature value (although for single crystal)[15] and the relative permittivity of BT to be 2500 and using the Maxwell Garnett equation 1:

$$\varepsilon_{comp} = \varepsilon_1 - \frac{3x_2\varepsilon_1(\varepsilon_1-\varepsilon_2)}{3\varepsilon_1-x_1(\varepsilon_1-\varepsilon_2)} \qquad \text{(eq. 1)}$$

where ε_{comp} is the permittivity of the 0-3 composite, x_1 and x_2 are volume fractions, and ε_1 and ε_2 are the relative permittivity of each phase. It follows ε_{comp}: 2146, 1823, 1529 and 1259 for 10, 20, 30 and 40 wt%, respectively. These values are higher than the experimental ones shown in Fig. 4. Instead, using the Lichtenecker equation[16]:

$$\ln \varepsilon_{comp} = (1 - x_2) \ln \varepsilon_1 + x_2 \ln \varepsilon_2 \qquad \text{(eq. 2)}$$

By using the same values for ε_1 and ε_2 we obtain the following results for ε_{comp}, for increasing YIG contents: 1489, 886, 528 and 314. This equation is in good agreement for 10 and 40 wt% YIG, but fails to account for the experimental value of permittivity for 20 and 30 wt%. The discrepancy between the predictions and the experimental values shows that the assumptions made for the Maxwell-Garnett or the Effective Medium Approximation (EMA) model were not fulfilled in the real case. Basically, the microstructures are not standard EMA ones. Hence, there are possible interactions among embedded particles, or particles may have different sizes and shapes. It was demonstrated that the Lichtenecker logarithmic expression characterises a specific microgeometry of a composite system only, which cannot be reduced neither to the Maxwell Garnett microgeometry, nor to that of Bruggemann[17]. For example, the Lichtenecker's equation also could explained to some extent the permittivity decay in PZT-ferrite ceramic composites when increasing the ferrite amount, but the best results could be provided by calculations with finite element methods using realistic microstructures[18].

The high field electrical measurements demonstrate that BT-YIG composites are electrically insulating up to 30 wt% YIG. For 40 wt% YIG instead, the maximum applicable electric field is limited to 15 kV/cm before short-circuit occurs, and it is evident from the shape of the polarisation curve, which appears due to conductivity rather than electrical polarisation. We can therefore conclude that the percolation limit lies between 30 and 40 wt% YIG in BT.

As far as magnetic properties are concerned, the value of saturation magnetisation for composites with YIG = 10-20 wt% is significantly below what one would expect by simply correcting for the YIG concentration. This discrepancy decreases for YIG concentrations ≥ 30 wt%, which are closer to the theoretical values. For the composite at lowest YIG concentration, coercivity is also significantly

higher than in the other composites and isolated YIG. From the shape of the hysteresis loops for all composites we can observe the absence of parasitic hard magnetic phases even for YIG = 40 wt%.

Lower ME coefficients (~24 to 60 μV cm^{-1} Oe^{-1}) for YIG-BT composites in comparison with the well-studied $CoFe_2O_4$-BT composites (~130 mV cm^{-1} Oe^{-1}) could have been partially anticipated, because YIG exhibits a magnetostriction coefficient (~ -3 ppm), which is two orders of magnitude lower than the magnetostriction coefficient for $CoFe_2O_4$ (~ -165 ppm). Nevertheless, it is still remarkable that a magnetoelectric response, yet low is obtained in the composites as a result of the partial poling. Moreover, as expected the ME coefficient increases with the YIG content. Recently, Wang et al[19] showed 0-3 type $BiY_2Fe_5O_{12}$-BT composites to exhibit an ME as high as 0.24 mV cm^{-1} Oe^{-1}. They also fabricated 2-2 type composites and measured a ME of 14.36 mV cm^{-1} Oe^{-1} at 600 Oe for a composite with 40 wt% of $BiY_2Fe_5O_{12}$ in BT. This value is becoming closer to the minimum of 20 mV cm^{-1} Oe^{-1} required for applications. Interestingly, the ME coefficients peak close to the saturating field for the M(H) response, which may be ascribed to the saturation of the magnetostrictive response of the YIG phase.

In summary, to date YIG-BT based composites have lower ME coefficients that other well-studied all-oxide multiferroic composites, however through improvements on processing, use of other geometries and chemical modifications, the performance of YIG-based composites may be improved to a point that they may afford useful properties for application.

Conclusions

Dense particulate multiferroic composites of ferrimagnetic YIG embedded into a matrix of ferroelectric BT were fabricated from precursors prepared by solid state reaction method. The ferroelectric and ferrimagnetic nature of the initial precursors was preserved in the composites. XRD patterns confirm the presence of YIG and tetragonal BT with little or no parasitic phases. Raman spectroscopy analysis confirms retention of ferroelectricity up to 40 wt% YIG included. Magnetic hysteresis loops also show the typical ferrimagnetic behaviour derived from the YIG parent phase. Finally, these dense ceramics can be partially poled, after which they exhibit a weak magnetoelectric

response, as partially expected from the low magnetostriction coefficient (-3 ppm) of YIG, in comparison with other magnetostrictive oxides such as $CoFe_2O_4$ (-165 ppm). Nevertheless, this ME coupling increases with YIG content. Recently it was demonstrated that doped YIG-BT laminated composites can exhibit ME coefficients as large as 14.36 mV cm^{-1} Oe^{-1}, which shows the potential for further improve YIG-based multiferroics.

Acknowledgements

This work was funded by the Christian Doppler Association in cooperation with TDK-EPC (Austria). LM acknowledges the grant PN-II-ID-PCE-2011-3-0745, while MA thanks funding by Spanish MINECO through project MAT2011-23709.

References

1. W. Eerenstein, N. D. Mathur, and J. F. Scott, "Multiferroic and magnetoelectric materials," *Nature*, 442[7104] 759-65 (2006).
2. J. F. Scott, "Data storage - Multiferroic memories," *Nature Materials*, 6[4] 256-57 (2007).
3. N. A. Hill, "Why are there so few magnetic ferroelectrics?," *Journal of Physical Chemistry B*, 104[29] 6694-709 (2000).
4. C.-W. Nan, M. I. Bichurin, S. Dong, D. Viehland, and G. Srinivasan, "Multiferroic magnetoelectric composites: Historical perspective, status, and future directions," *Journal of Applied Physics*, 103[3] (2008).
5. R. E. Newnham, D. P. Skinner, and L. E. Cross, "Connectivity and Piezoelectric-pyroelectric composites," *Materials Research Bulletin*, 13[5] 525-36 (1978).
6. G. Schileo, A. Feteira, I. M. Reaney, P. Postolache, L. Mitoseriu, and K. Reichmann, "Characterization of Yttrium Iron Garnet/Barium Titanate Multiferroic Composites Prepared by Sol-Gel and Coprecipitation Methods," *International Journal of Applied Ceramic Technology*, 11[3] 457-67 (2014).
7. L. Fernandez-Garcia, M. Suarez, and J. L. Menendez, "Synthesis of mono and multidomain YIG particles by chemical coprecipitation or ceramic procedure," *Journal of Alloys and Compounds*, 495[1] 196-99 (2010).
8. C. H. Perry and D. B. Hall, "Temperature Dependence of the Raman Spectrum of $BaTiO_3$" *Physical Review Letters*, 15[17] 700-02 (1965).
9. M. Acosta, N. Liu, M. Deluca, S. Heidt, I. Ringl, C. Dietz, R. Stark, and W. Jo, "Tailoring ergodicity through selective A-site doping in the $Bi_{1/2}Na_{1/2}TiO_3$-$Bi_{1/2}K_{1/2}TiO_3$ system," *Journal of Applied Physics*, 117[13] (2015).
10. G. Schileo, L. Luisman, A. Feteira, M. Deluca, and K. Reichrnann, "Structure-property relationships in $BaTiO_3$-$BiFeO_3$-$BiYbO_3$ ceramics," *Journal of the European Ceramic Society*, 33[8] 1457-68 (2013).
11. D. Schuetz, M. Deluca, W. Krauss, A. Feteira, T. Jackson, and K. Reichmann, "Lone-Pair-Induced Covalency as the Cause of Temperature- and Field-Induced Instabilities in Bismuth Sodium Titanate," *Advanced Functional Materials*, 22[11] 2285-94 (2012).
12. D. Ghosh, H. Han, J. C. Nino, G. Subhash, and J. L. Jones, "Synthesis of $BaTiO_3$-20wt%$CoFe_2O_4$ Nanocomposites via Spark Plasma Sintering," *Journal of the American Ceramic Society*, 95[8] 2504-09 (2012).

13. D. V. Karpinsky, R. C. Pullar, Y. K. Fetisov, K. E. Kamentsev, and A. L. Kholkin, "Local probing of magnetoelectric coupling in multiferroic composites of $BaFe_{12}O_{19}$-$BaTiO_3$," *Journal of Applied Physics,* 108[4] (2010).
14. J. Nie, G. Xu, Y. Yang, and C. Cheng, "Strong magnetoelectric coupling in $CoFe_2O_4$-$BaTiO_3$ composites prepared by molten-salt synthesis method," *Materials Chemistry and Physics,* 115[1] 400-03 (2009).
15. M. A. Popov, I. V. Zavislyak, and G. Srinivasan, "Sub-THz dielectric resonance in single crystal yttrium iron garnet and magnetic field tuning of the modes," *Journal of Applied Physics,* 110[2] (2011).
16. T. Kondo and S. Yoshikado, "Electromagnetic characteristics of a ceramic composite," *Journal of the Ceramic Society of Japan,* 109[4] 326-31 (2001).
17. A. V. Goncharenko, V. Z. Lozovski, and E. F. Venger, "Lichtenecker's equation: applicability and limitations," *Optics Communications,* 174[1-4] 19-32 (2000).
18. C. E. Ciomaga, C. S. Olariu, L. Padurariu, A. V. Sandu, C. Galassi, and L. Mitoseriu, "Low field permittivity of ferroelectric-ferrite ceramic composites: Experiment and modeling," *Journal of Applied Physics,* 112[9] (2012).
19. F. Wang, G. Zhang, H. Yang, M. Liu, and Y. Yang, "Low temperature sintering and magnetoelectric properties of laminated $BaTiO_3$/$BiY_2Fe_5O_{12}$ composites," *Journal of Alloys and Compounds,* 632 460-66 (2015).

List of Figures

List of Tables

		x=0 %wt (BT)	x=10 %wt	x=20 %wt	x=30 %wt	x=40 %wt	x=100 %wt (YIG)
BT	**a (Å)**	3.9906(1)	3.9970(2)	4.0000(1)	3.9979(3)	3.9968(1)	
	c (Å)	4.0330(1)	4.0219(3)	4.0152(3)	4.0186(4)	4.0130(2)	
	c/a	1.0106	1.0062	1.0038	1.0052	1.0041	
YIG	**a (Å)**		17.496(1)	17.493(8)	17.483(2)	17.4925(5)	17.5021(6)
	c (Å)		10.691(3)	10.720(1)	10.716(4)	10.7007(5)	10.7244(7)

Table 1. Lattice parameters for BT, YIG and BT-YIG composites (10 %wt ≤ x ≤ 40 %wt) sintered at 1300 ºC for 2 h.

Figures

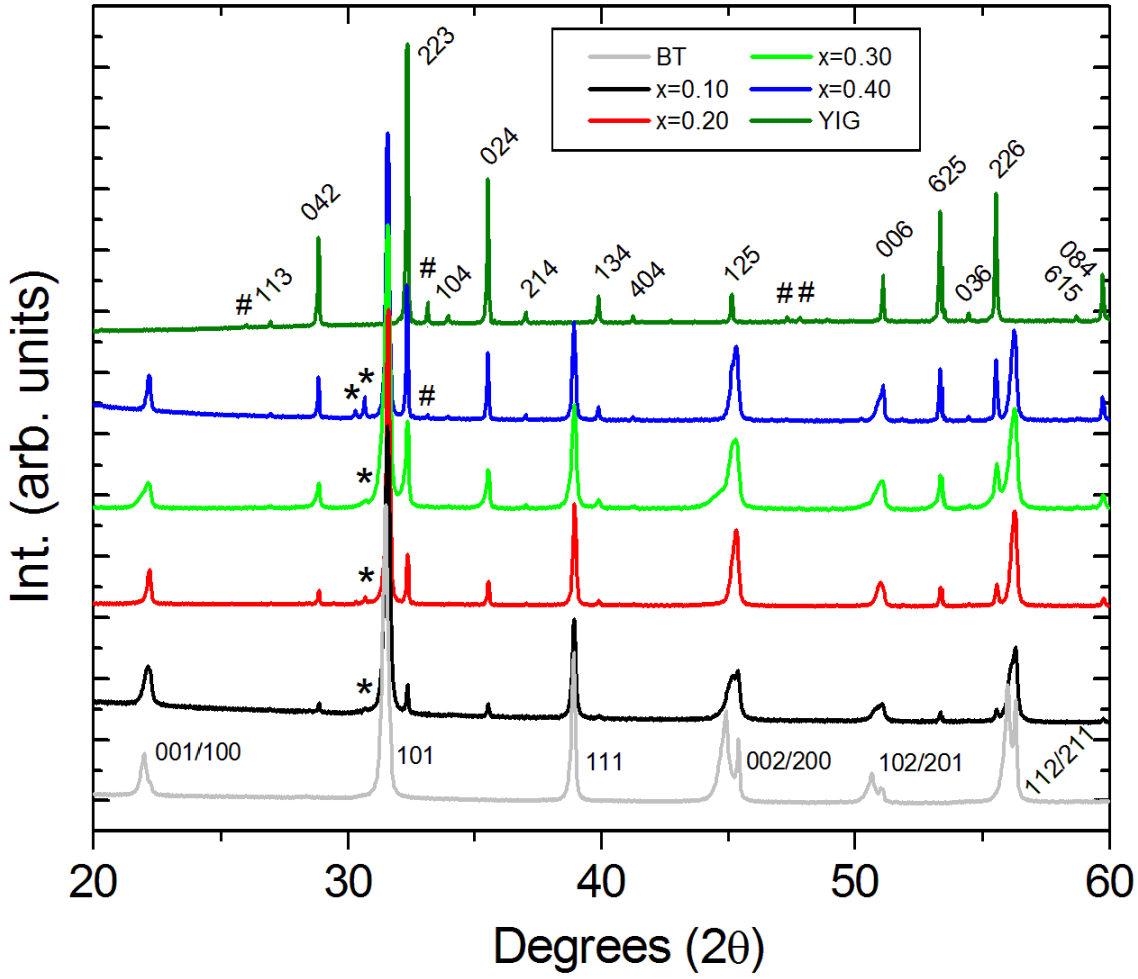

Figure 7. Room temperature x-ray diffraction data of BT, BT-YIG composites with YIG concentration ranging from 10 %wt to 40 %wt, and YIG sintered at 1300 °C for 2 h (# = $YFeO_3$, * = $Y_2Ti_2O_7$ and/or $BaFe_{12}O_{19}$) (from bottom to top)

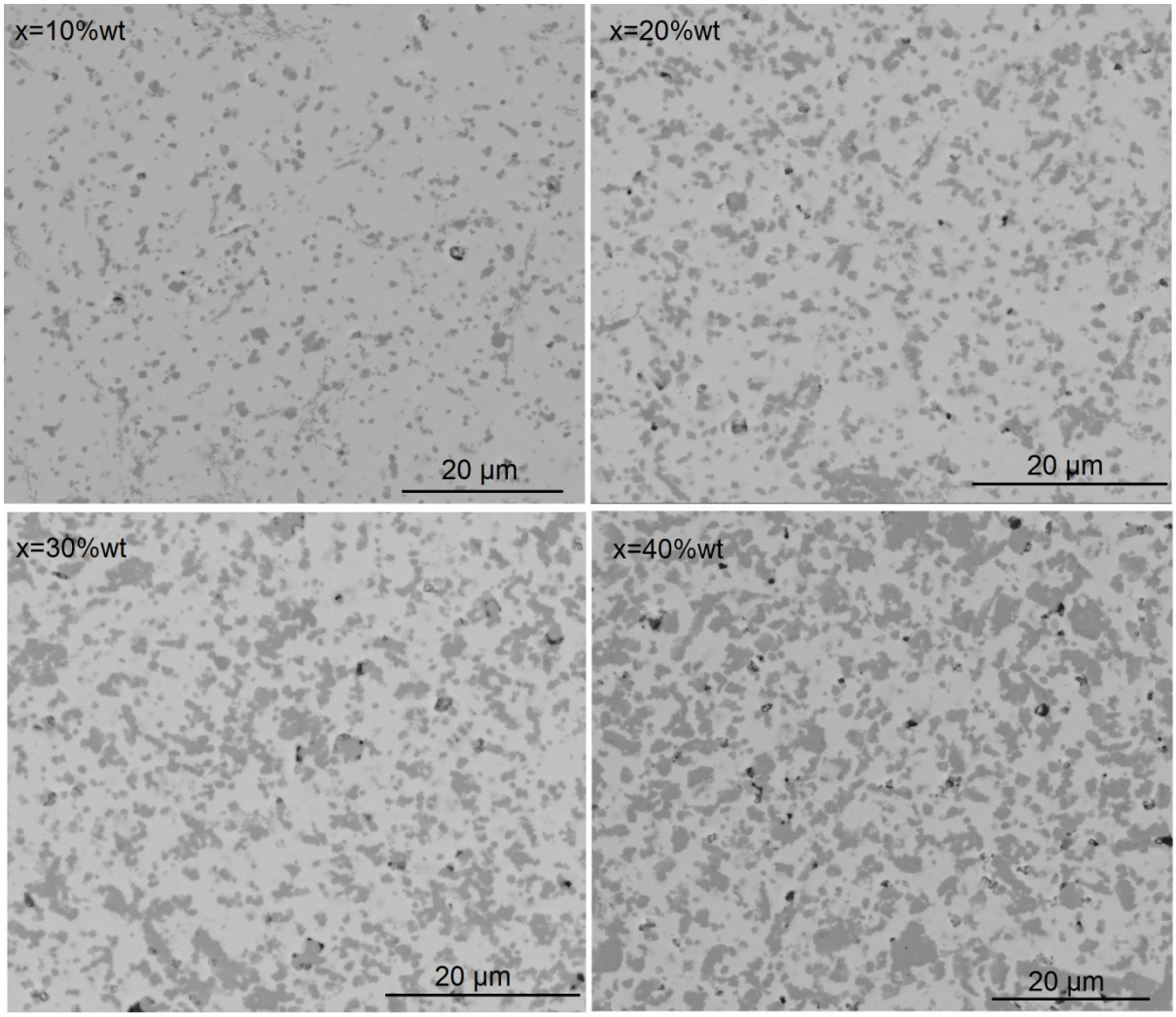

Figure 8. Back-scattering SEM images showing the typical microstructure of ceramic composites with increasing concentration of YIG, sintered at 1300 ºC for 2 h.

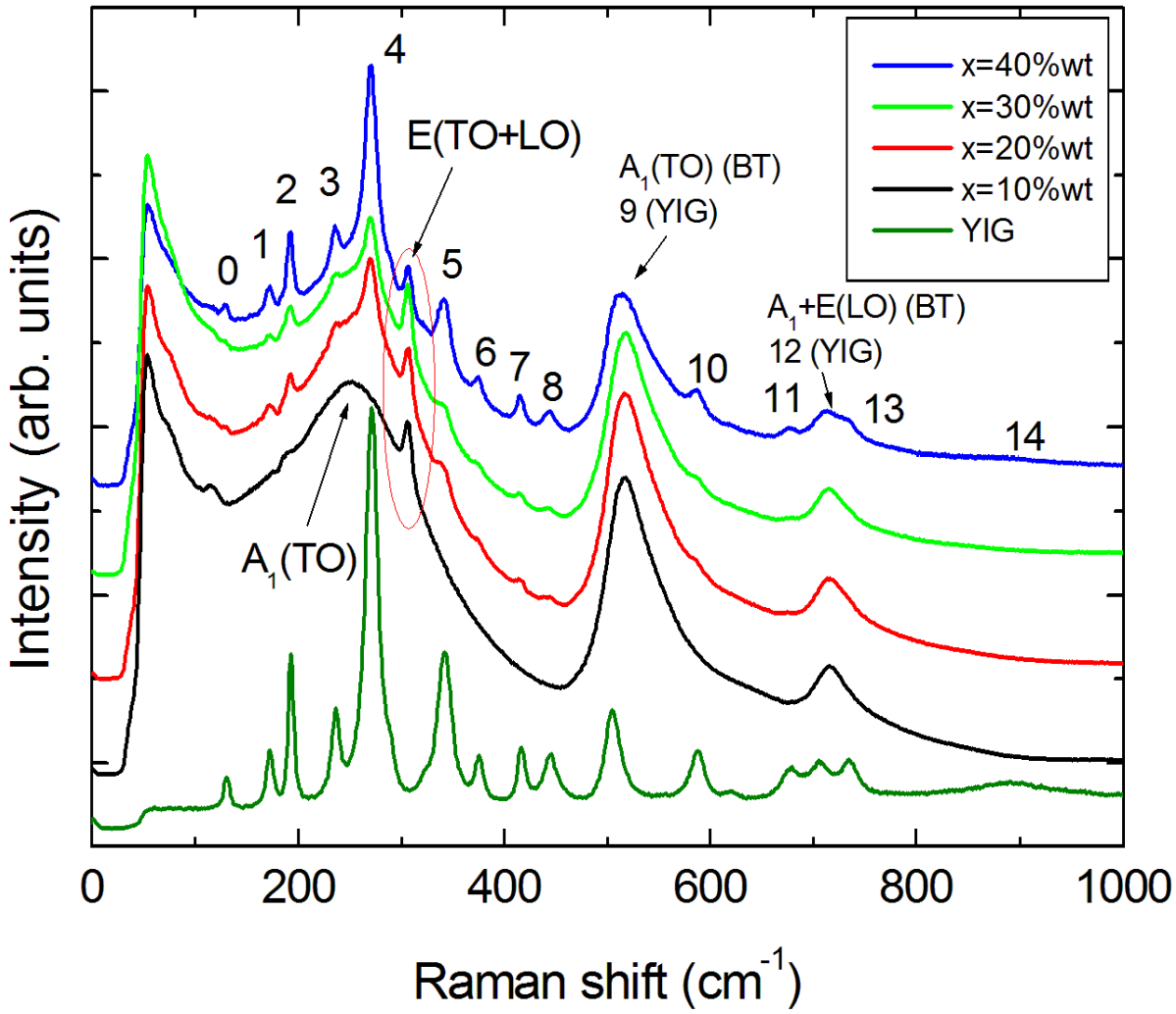

Figure 9. Raman spectra of YIG and BT-YIG composites with YIG concentration ranging from 10 %wt to 40 %wt. Spectra were collected on polished surfaces of pellets sintered at 1300 ºC for 2 h (from bottom to top).

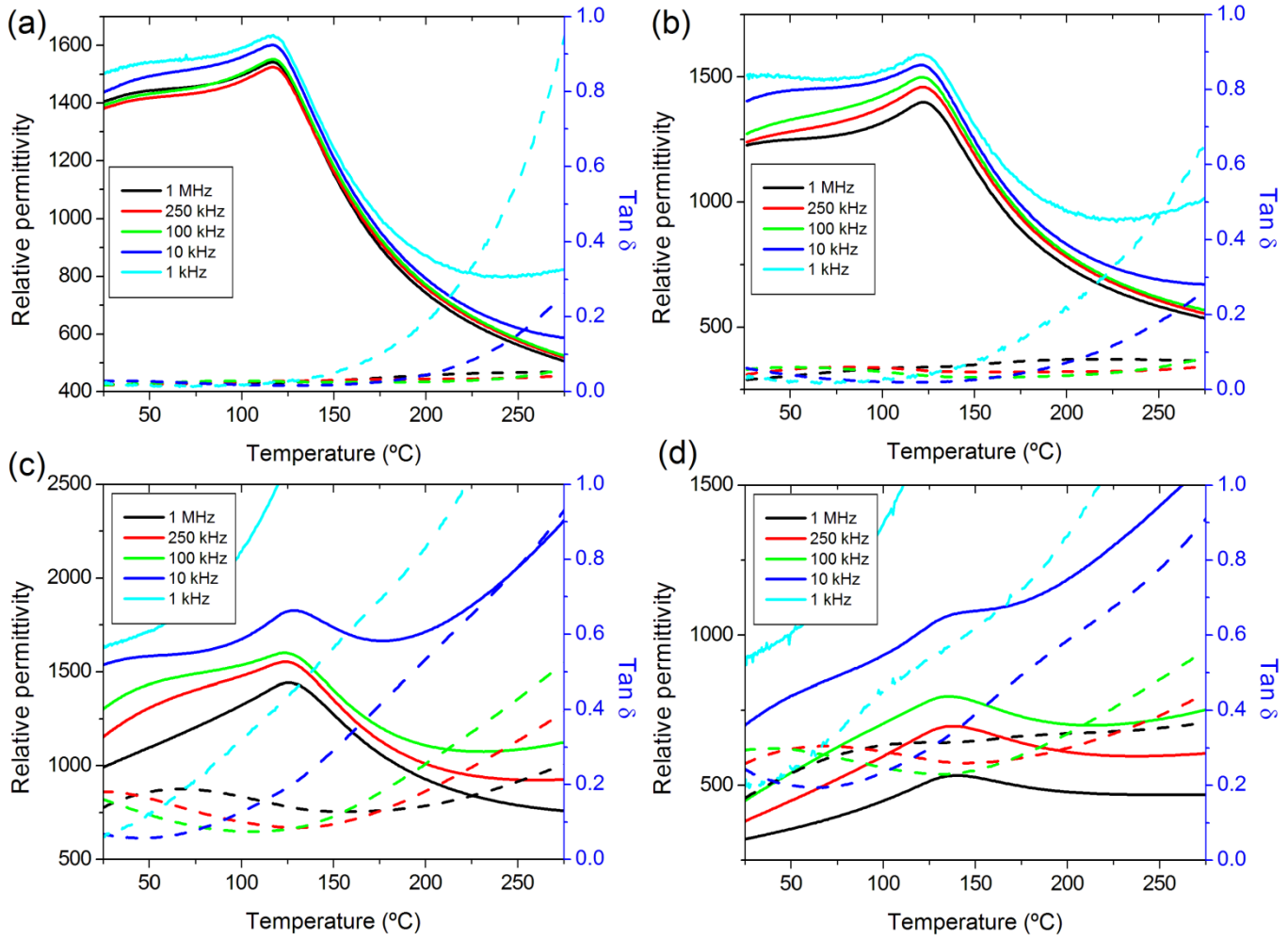

Figure 10. Temperature dependence of relative permittivity and dielectric loss for composites with a) 10 %wt, b) 20 %wt, c) 30 %wt, and d) 40 %wt YIG in BT.

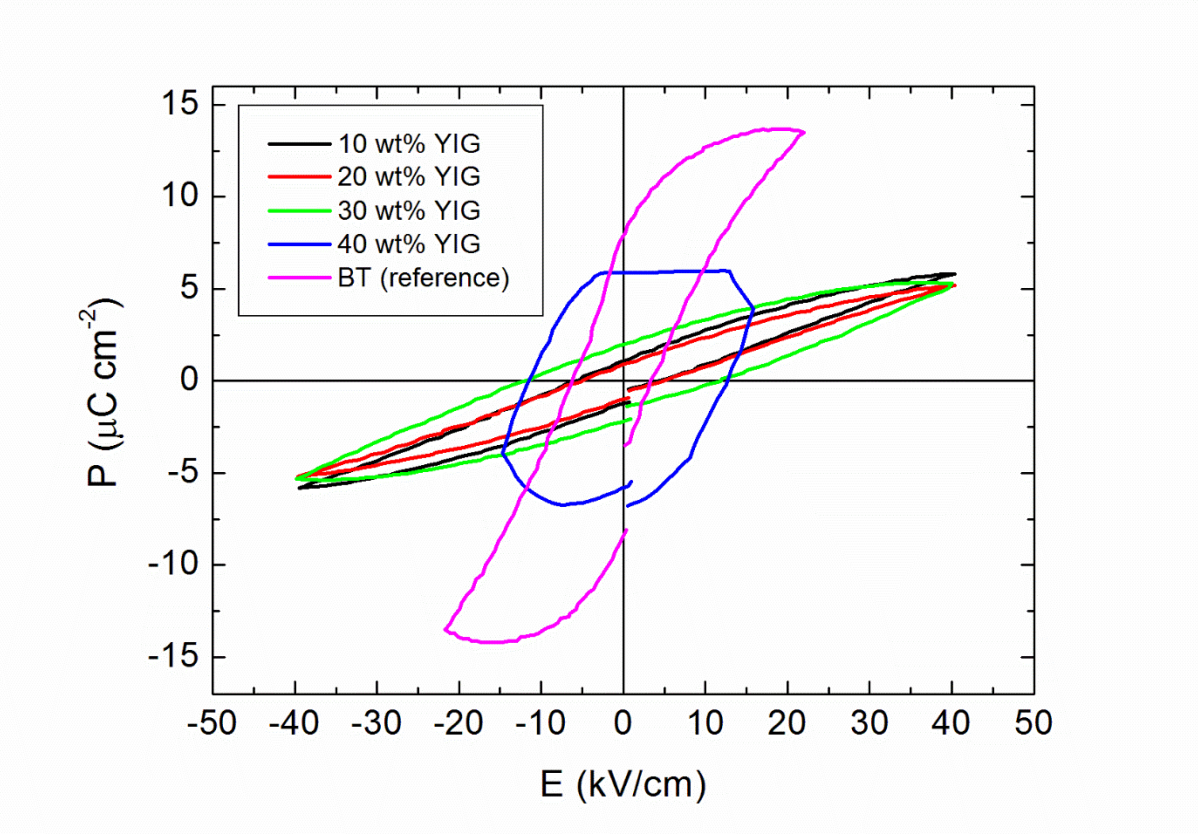

Figure 11. Ferroelectric hysteresis loops for BT-YIG ceramic composites.

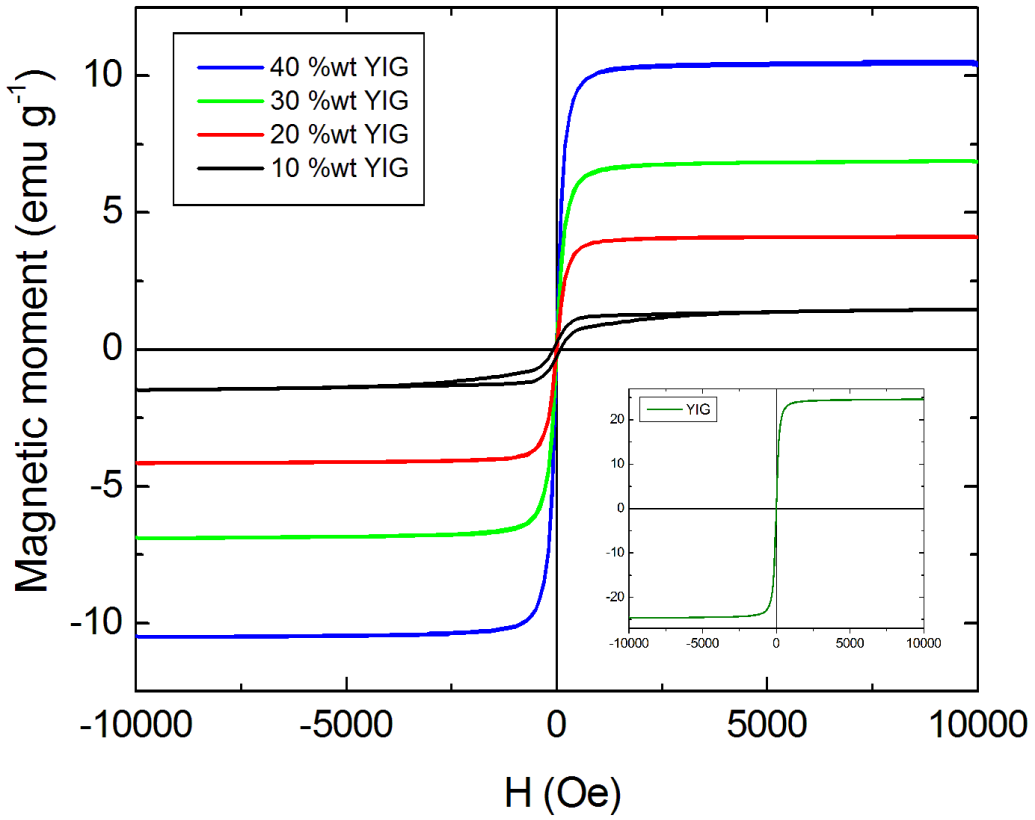

Figure 12. Magnetic hysteresis loops for BT-YIG composites; inset: magnetic hysteresis loop for YIG.

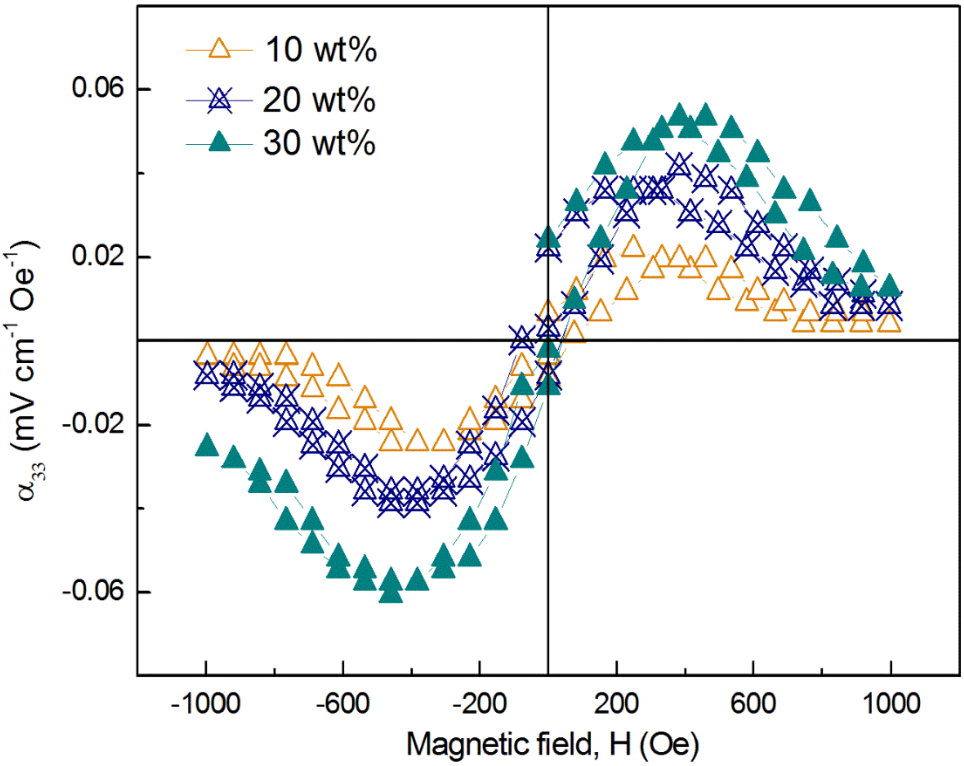

Figure 7. Magnetoelectric coefficients for BT-YIG composites.